ELECTRODE PERFORMANCES OF MELT-SPINNED AB_2 TYPE Zr-BASED HYDROGEN STORAGE ALLOYS①

Yang Xiaoguang, Shu Kangyin, Zhang Xiaobin, Lei Yongquan and Wang Qidong
Department of Materials Science and Engineering, Zhejiang University, Hangzhou 310027, P. R. China
Zhang Wenkui
Department of Applied Chemistry, Zhejiang University of Technology, Hangzhou 310014, P. R. China
Lü Guanglie
Central Laboratory, Hangzhou University, Hangzhou 310028, P. R. China

ABSTRACT Effect of rapid solidification on electrochemical properties and the microstructure of AB_2 type Zr-based alloy was reported. The electrochemical capacity of $ZrCr_{0.4}Mn_{0.2}V_{0.1}Ni_{1.2}Fe_{0.1}$ melt-spinning alloy sharply decreased and the activating process prolonged in comparison with that of arc-melt ones. XRD analyses revealed that the lattice parameter of C15 main phase in melt-spinning alloy shrinks obviously, and alloy ribbon is covered by a ZrO_2 layer. Extra fine microstructure (grain size about 125 nm) and high-density planar defects were detected by TEM observation. A smaller lattice cell and lack of Zr_7M_{10} are regarded to depress the electrochemical properties of the melt-spinning alloy.

Key words Zr-based hydrogen storage alloy rapid solidification electrode performances

1 INTRODUCTION

It is assumed that the electrochemical properties depend on both the chemical composition and the microstructure of hydrogen storage alloys. Many researches have been reported that the main properties, such as electrochemical capacity, high-rate dischargeability, resistance to anodic oxidation and cyclic life have been modified by alloying treatment[1-3]. For a hydrogen storage alloy with a certain composition, the foresaid properties can be modified by altering its microstructure[4-6]. Mishima *et al*[7] surveyed the electrochemical properties of the rapidly solidified alloy $LaNi_{4.6}Al_{0.4}$ prepared by a melt-spinning method. It was found that melt-spinning alloy exhibited a longer cyclic life than that of its master alloy produced by conventional melting (after 100 cycles at 20 ℃) because the former has a finer grain size (1~ 2 μm) than that (20~ 30 μm) of the later. Lei[8] reported that unidirectionally solidified alloy $Ml(NiCoMnTi)_5$ (Ml: La-rich mischmetal) with fine cellular-columnar structure prepared at an ultra-high temperature gradient (about 1 300 ℃/cm) and growth rate (R= 48 μm/s) has significantly improved the discharge capacity, high-rate dischargeability and cycling stability. For AB_2 type Laves phase hydrogen storage alloys, the discharge capacity of $ZrCr_{0.4}Mn_{0.2}V_{0.1}Ni_{1.3}$ was found to decrease sharply from 324 mAh/g to 25 mAh/g after amorphism process by mechanically milling the crystalline (as-cast) alloy with stainless steel balls. Hydrogen atoms stored in half tetrahedral interstices of Zr_2B_2(B= Cr, V or Ni) contribute to its electrochemical capacity for as-cast alloy, while the hydrogen atoms in half sites of Zr_3B and Zr_4 in ball-milling amorphous alloy do. The extra energy stored during milling process is released to lower the barrier potential for

① Project 863-715-004-0060 supported by the National Advanced Materials Committee of China and project 59601006 supported by the National Natural Science Foundation of China Received Dec. 29, 1997; accepted Mar. 23, 1998

the hydrogen discharge reaction by about 60 kJ·mol^{-1} H^{-1}[4].

In the present paper, the authors conducted the rapidly solidified method on the AB_2 type $ZrCr_{0.4}Mn_{0.2}V_{0.1}Ni_{1.2}Fe_{0.1}$ alloy and investigated its effect on the electrochemical properties and observed the alloy microstructure by TEM as well.

2 EXPERIMENTAL DETAIL

The $ZrCr_{0.4}Mn_{0.2}V_{0.1}Ni_{1.2}Fe_{0.1}$ alloy was firstly prepared by arc melting under argon atmosphere and re-melted for several times. The as-cast ingot was re-melted in a spinning machine to produce the ribbons under 70 kPa Ar with a Cu roll (20 cm in diameter, rotating rate of 1 500 r/min). The ribbons are of 50 μm in thickness and 2 mm in width. Both alloys in as-cast state and in rapidly solidified state were crushed mechanically in air.

Powder X-ray diffraction data were obtained from sieved grains (< 46 μm) of these different inactivated alloys or the ribbon using Rigaku C-max-III B diffractometer with a Cu K_α radiation and a nickel diffracted-beam filter. TEM observation was performed on JEOL JEM-100CX II microscopy.

The preparation of test electrode was described as previously reported[3]. Electrochemical measurements were carried out in a trielectrode electrolysis cell, in which the counter-electrode was nickel oxyhydroxide, reference electrode was Hg/HgO/KOH(6 mol·L^{-1}), and the electrolyte was 6 mol/L KOH solution. The discharge capacities of hydride electrodes were determined by galvanostatic method. The electrodes were fully charged at a current density of 100 mA/g and discharged at 50 mA/g. The cut-off potential was set to − 0.6 V vs Hg/HgO.

3 RESULTS AND DISCUSSION

Fig. 1 shows the initial discharge capacity change of the as-cast and melt-spinning alloy electrodes $ZrCr_{0.4}Mn_{0.2}V_{0.1}Ni_{1.2}Fe_{0.1}$. Both electrodes have no ability to discharge proton on the initial cycling stage. The as-cast electrode exhibits a capacity of 215 mAh/g on the 5th cycling, and reaches its maximal discharge capacity of 320 mAh/g after 19 cyclings. However the electrode prepared from melt-spinning alloy needs a much longer cycling process (about 60 cyclings) to reach its maximal capacity of 51 mAh/g, only 1/6 that of the master alloy. There exists apparent variation in capacity property between the as-cast and melt-spinning alloy electrodes.

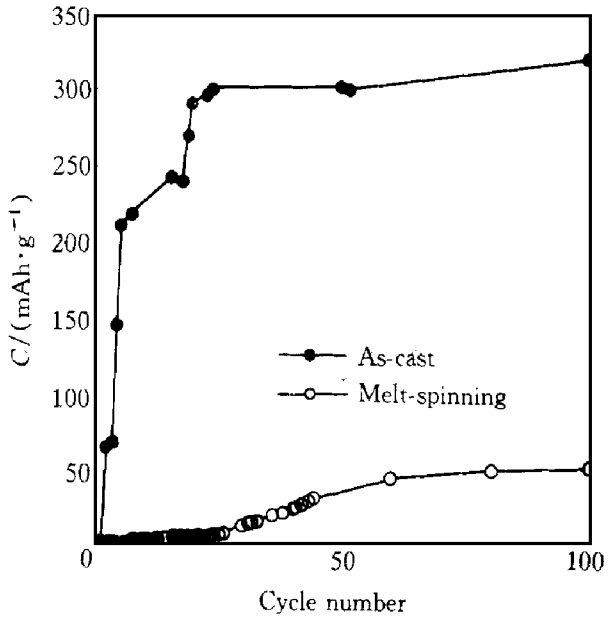

Fig. 1 Activating processes of two kinds $ZrCr_{0.4}Mn_{0.2}V_{0.1}Ni_{1.2}Fe_{0.1}$ alloys
(Discharge current density 50 mA/g, 298 K)

Fig. 2 depicts the XRD patterns of as-cast, melt-spinning alloy powder and its ribbon of $ZrCr_{0.4}Mn_{0.2}V_{0.1}Ni_{1.2}Fe_{0.1}$ alloys. The as-cast alloy consists of a fcc C15 Laves main phase, a small amount of hcp C14 Laves phase and other pseudo-binary phases Zr_7M_{10} and Zr_9M_{11} (M = Cr, Mn, V, Fe and Ni). The melt-spinning alloy is of C15 main phase too, but the C14 phase has a tendency to be amorphous, which is verified by broadening of XRD peaks of C14 phase shown in Fig. 2(b) or 2(c). The authors suggest that the C14 phase alloy possibly solidifies firstly and transmits to an amorphous alloy under a larger cooling gradient. The C14 phase usually contains more Cr, V or Mn element instead of Ni in the B-side. Pseudo-binary phases Zr_7M_{10}

and Zr_9M_{11} are found to disappear in the melt-spinning alloy as well.

The main phase C15 remains in a good crystalline state in the melt-spinning alloy because of its narrow diffraction peaks. There is no obvious discrepancy in their XRD patterns detected from powder and ribbon of melt-spinning alloys except the peak at $2\theta = 30°$, which is identified as the strongest one of ZrO_2. The high oxide peak indicates that the ribbon is covered by an oxide layer with certain thickness.

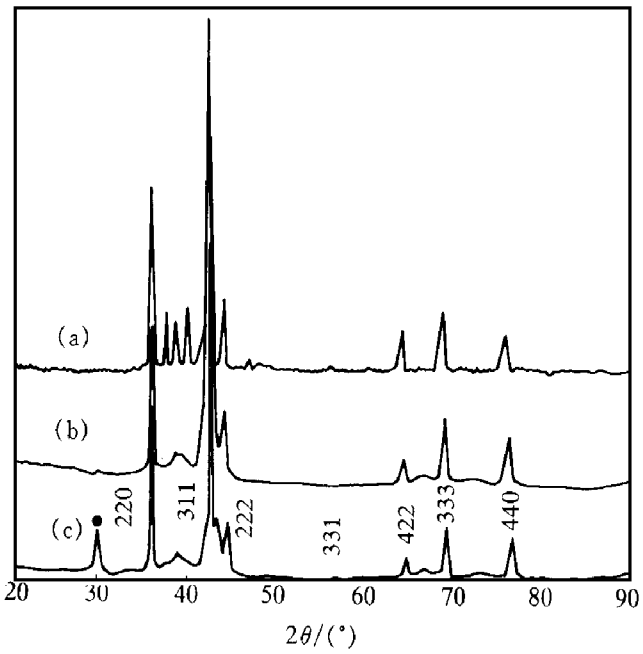

Fig. 2 XRD patterns of $ZrCr_{0.4}Mn_{0.2}V_{0.1}Ni_{1.2}Fe_{0.1}$ alloy under different conditions
(a) —As-cast alloy;
(b) —Melt-spinning powdered alloy;
(c) —Melt-spinning ribbons

Furthermore, the value (d) of diffraction peak indexed (311) of main phase C15 is found to vary from $d = 0.2128$ nm in as-cast to 0.2118 nm in rapidly solidified state. The lattice parameter of melt-spinning alloy decreases and its cell volume shrinks by 1.4%. In the electrochemical test, the as-cast master alloy exhibits a good electrochemical capacity of 320 mAh/g at room temperature. This implies that the hydride in as-cast electrode has suitable thermodynamics stability, accompanying a suitable lattice parameter. With the same chemical atomic environment, the absorbing/desorbing hydrogen capacity of the melt-spinning alloy flags rationally since it has a contracted lattice parameter[2].

Fig. 3 depicts the TEM micrograph of the melt-spinning alloy. We can see that its microstructure is extremely fine with a grain size of about 125 nm. There are many bright and dark strings within grains, which implies that abundant planar defects exist. Meanwhile some white small spheres are also found to disperse throughout the observing area, which is presumed to be ZrO_2 spheres induced during the melting process.

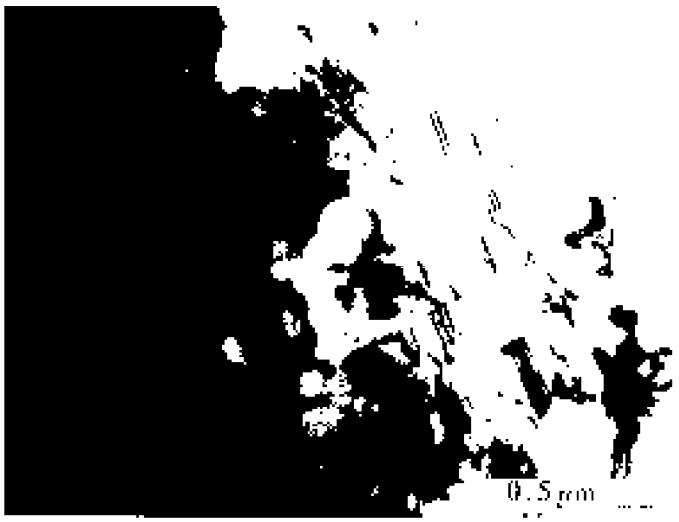

Fig. 3 Morphology of melt-spinning $ZrCr_{0.4}Mn_{0.2}V_{0.1}Ni_{1.2}Fe_{0.1}$ alloy

There are two points worth discussing further. The first is a notable degradation in the activation of the melt-spinning $ZrCr_{0.4}Mn_{0.2}V_{0.1}Ni_{1.2}Fe_{0.1}$ electrode. From the results of XRD, an outer oxide layer with a certain thickness is confirmed. The melt-spinning alloy is found to have a smaller grain size of about 125 nm. The finer microstructure makes the bulk flexible and suppresses the pulverization because the grain boundaries could work as a buffer region for releasing lattice strain, thus the activation process is rationally hindered.

Sawa *et al*[9] regarded that the activation process of Zr-based hydride electrodes accompanied a structure transformation of outer layer from monoclinic to tetragonal ZrO_2. However, the present paper reveals that the inactivated melt-spinning alloy is just covered by a tetragonal

oxide. Based on the reason above mentioned, a conclusion is drawn that the structure change of the oxide layer might not be the basic factor determining its activation process. The physical properties such as the compactness are more important. In addition, the component Cr would make a negative effect on activation as well.

The other is a sharp drop in discharge capacity by about 83%. One reason is the shrinking in cell volume of the main phase C15. While Mishima *et al*[7] have discovered that the hydrogen storage capacity of melt-spinning $LaNi_{4.6}Al_{0.4}$ alloy also decreased to some extent in comparison with that of conventional melting ones. Meanwhile, some pseudo-binary alloys Zr_7M_{10} and Zr_9M_{11} are found to disappear in melt-spinning alloy. The precipitation of Zr_7M_{10} is regarded to be the necessary catalytic sites for the electrochemical reaction[10]. Lack of Zr_7M_{10} phase will decrease the discharge capacity of melt-spinning alloy because of the sluggish discharge kinetics.

4 CONCLUSIONS

The electrochemical capacity of the $ZrCr_{0.4}Mn_{0.2}V_{0.1}Ni_{1.2}Fe_{0.1}$ melt-spinning hydride electrode decreases sharply from 321 mAh/g of its arc-melting master alloy to 50 mAh/g, and the activating process prolongs. By XRD analyses, it is found that the main phase lattice parameter (a) of the melt-spinning alloy recoils without change in spatial structure, and that the alloy ribbon is covered by a thin ZrO_2 layer. The fine microstructure (a grain size of about 125 nm) and high-density planar defects are detected by TEM. A smaller lattice cell and lack of Zr_7M_{10} are regarded to depress the electrochemical properties of the melt-spinning alloy.

REFERENCES

1 Zuettel A, Meli F and Schlapbaph L. J Alloys and Comp, 1994, 203: 235.
2 Lei Y Q. Yang X G, Wu J *et al*. J Alloys and Comp, 1995, 231: 573.
3 Yang X G, Lei Y Q, Chen Y L *et al*. Trans Nonferrous Met Soc China, 1997, 7(3): 1.
4 Yang X G, Lei Y Q, Zhang W K *et al*. Acta Metall Sinica, (in Chinese), 1996, 32: 1192.
5 Sakai T, Yoshinaga H, Miyamura H *et al*. J Alloys and Comp, 1992, 180: 37.
6 Notten P H L and Einerhand R E F. Adv Mater, 1991, (3): 343.
7 Mishima R, Miyamura H, Sakai T *et al*. J Alloys and Comp, 1993, 192: 176.
8 Lei Y Q, Zhou Y, Luo Y C *et al*. J Alloys and Comp, 1997, 253– 254: 590.
9 Sawa H, Ohta M, Nakao H *et al*. Z Fur Physik Chemie, 1989, 164: 1527.
10 Joubert J M, Latroche M, Percheron-Guegan A *et al*. J Alloys and Comp, 1996, 230: 100.

(Edited by Huang Jinsong)